10-1-2018

Small Shelly Fossil Preservation and the Role of Early Diagenetic Redox in the Early Triassic

Sara B. Pruss
Smith College, spruss@smith.edu

Nicholas J. Tosca
University of Oxford

Courcelle Stark
Smith College

Recommended Citation

SMALL SHELLY FOSSIL PRESERVATION AND THE ROLE OF EARLY DIAGENETIC REDOX IN THE EARLY TRIASSIC

Authors: PRUSS, SARA B., TOSCA, NICHOLAS J., and STARK, COURCELLE

PALAIOS

Emphasizing the impact of life on
Earth's history

SEPM
Society for
Sedimentary Geology

SMALL SHELLY FOSSIL PRESERVATION AND THE ROLE OF EARLY DIAGENETIC REDOX IN THE EARLY TRIASSIC

SARA B. PRUSS,[1] NICHOLAS J. TOSCA,[2] AND COURCELLE STARK[1]

[1]*Department of Geosciences, Smith College, Northampton, Massachusetts 01063, USA*
[2]*Department of Earth Sciences, University of Oxford, Oxford, OX1 3AN, UK*
email: spruss@smith.edu

ABSTRACT: Minute fossils from a variety of different metazoan clades, collectively referred to as small shelly fossils, represent a distinctive taphonomic mode that is most commonly reported from the Cambrian Period. Lower Triassic successions of the western United States, deposited in the aftermath of the end-Permian mass extinction, provide an example of small shelly style preservation that significantly post-dates Cambrian occurrences. Glauconitized and phosphatized echinoderms and gastropods are preserved in the insoluble residues of carbonates from the Virgin Limestone Member of the Moenkopi Formation. Echinoderm plates, spines and other skeletal elements are preserved as stereomic molds; gastropods are preserved as steinkerns. All small shelly style fossils are preserved in the small size fractions of the residues (177 to 420 µm), which is consistent with the size selection of small shelly fossils in the Cambrian. Energy-dispersive X-ray spectra of individual fossils coupled with X-ray diffraction of residues confirm that the fossils are dominantly preserved by apatite and glauconite, and sometimes a combination of the two minerals. The nucleation of both of these minerals requires that pore water redox oscillated between oxic and anoxic conditions, which, in turn, implies that Lower Triassic carbonates periodically experienced oxygen depletion after deposition and during early diagenesis. Long-term oxygen depletion persisted through the Early Triassic, creating diagenetic conditions that were instrumental in the preservation of small shelly fossils in Triassic and, likely, Paleozoic examples.

INTRODUCTION

Small shelly style preservation is a common mode of preservation in Cambrian deposits worldwide (Brasier 1990; Dzik 1994; Porter 2004). This style of preservation is characterized by the replacement of skeletal elements, regardless of taxonomic affinity, by apatite and to a lesser extent iron oxides and glauconite (e.g., Brasier 1990; Porter 2004; Creveling et al. 2014a, 2014b). These fossils have been well studied from insoluble residues of limestone, and it has been noted that the small size of some of these fossils is a function of the taphonomic process that fostered their preservation (Creveling et al. 2014b). For example, it has been suggested that the small size of the organisms likely led to the trapping of phosphorous-rich organic matter in the interstices of the shells, in an environment experiencing periodic oxygen depletion (Creveling et al. 2014b), at least in one Cambrian succession. Small shelly style preservation is present in the Ordovician (Dattilo et al. 2016) and into the Silurian (Dzik 1994) but their abundance declines after the early Cambrian (Porter 2004), and they are essentially absent from post-Paleozoic deposits (Dzik 1994).
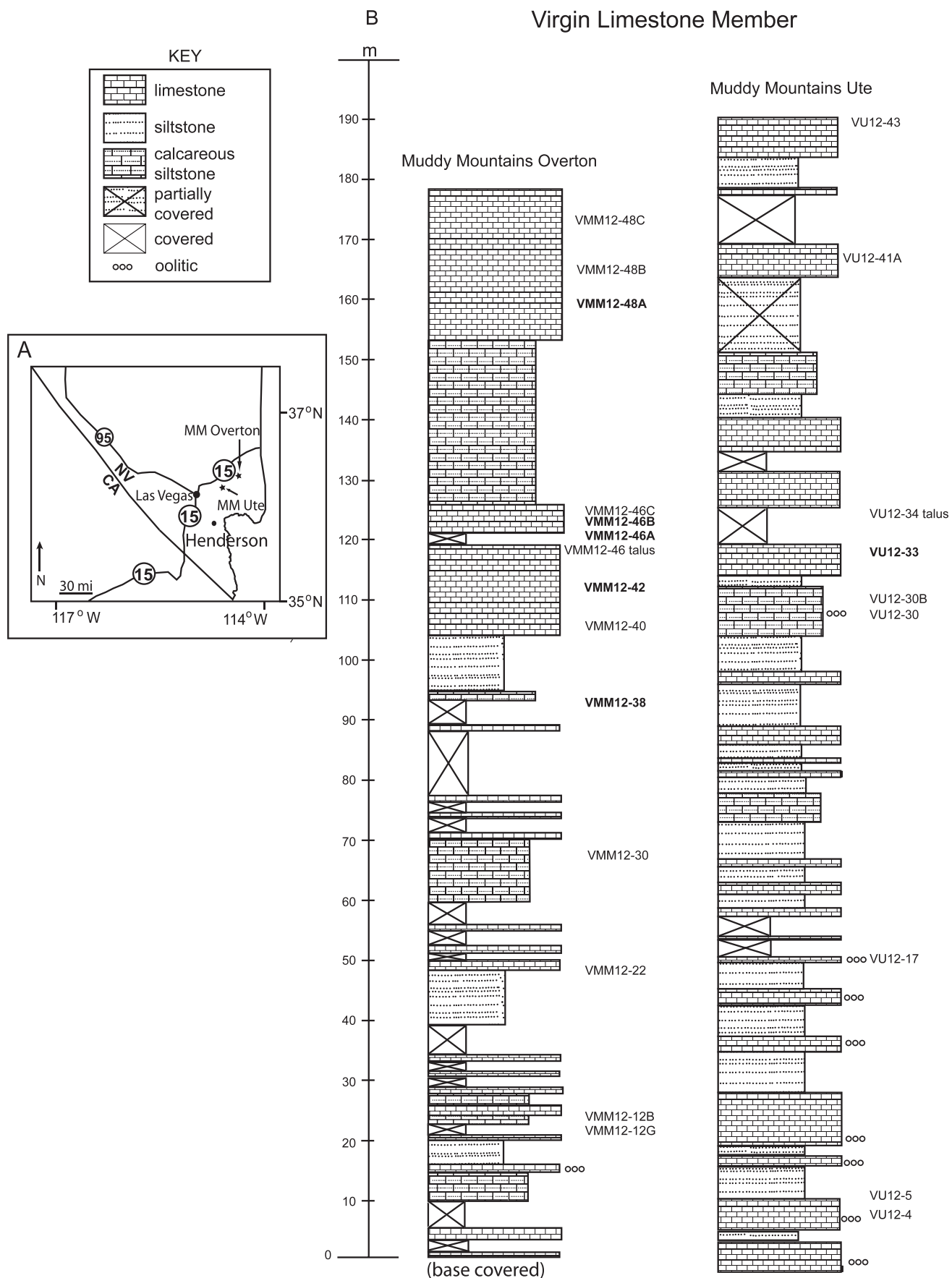
The composition of small shelly fossil assemblages changes through the Paleozoic (Dzik 1994). Early Cambrian assemblages are characterized by a variety of diminutive organisms and remains, some with problematic affinities, which make up the small shelly faunas (SSF) of this time. Many of these fossils are only known from their phosphatic remnants. In contrast, even by Ordovician time, much of what makes up phosphatized assemblages is also at least broadly reflected in the macrofaunal assemblage, but what appears to constrain phosphatization is the size of the organisms (Dattilo et al. 2016). Mollusks are common components of post-Cambrian assemblages, with small adults or juveniles making up much of what is preserved (Dzik 1994; Dattilo et al. 2016).

The decline in abundance of small shelly fossils, and relatedly, phosphatized deposits, after the Cambrian has been linked to the closing of a taphonomic window that operated in the early Paleozoic (Porter 2004). This disappearance coincides with seafloor settings becoming more oxygenated (Sperling et al. 2015), not unlike the distribution of soft-bodied fossils (Allison and Briggs 1993). However, despite the inference that anoxia played an important role in phosphatization, the geochemical mechanisms behind small shelly style preservation have remained unclear (e.g., Creveling et al. 2014b).

Here, we report a new assemblage of replaced fossils and internal molds in the small size fractions (250 µm to 420 µm; 177 µm to 250 µm) of residues that previously produced silicified fossils (Pruss et al. 2015) from the Lower Triassic (Spathian) Virgin Limestone Member, Moenkopi Formation of southern Nevada (Figs. 1, 2). Most of these fossils are glauconitic and phosphatic echinoderms and gastropods (Figs. 2–4); they are identical in mineralogy to many small shelly fossils of the Cambrian. The presence of these fossils in the small size fraction suggests that some Triassic deposits represent a resurgence of Cambrian-style preservation driven by prevailing redox conditions in the sediment during early diagenesis.

GEOLOGIC SETTING

In the Muddy Mountains of southern Nevada, the Spathian (upper Lower Triassic) Moenkopi Formation unconformably overlies the carbonates of the Lower Permian Kaibab Formation. The Moenkopi contains a series of fluvial-marine siliciclastic units with a few dominantly carbonate members (Shorb 1983). One such example of marine deposition is the Virgin Limestone Member (180 to 190 m-thick), a mixed carbonate-siliciclastic unit, which is well exposed in the Weiser Ridge near Overton,

B

Virgin Limestone Member

KEY
- limestone
- siltstone
- calcareous siltstone
- partially covered
- covered
- ooo oolitic

A

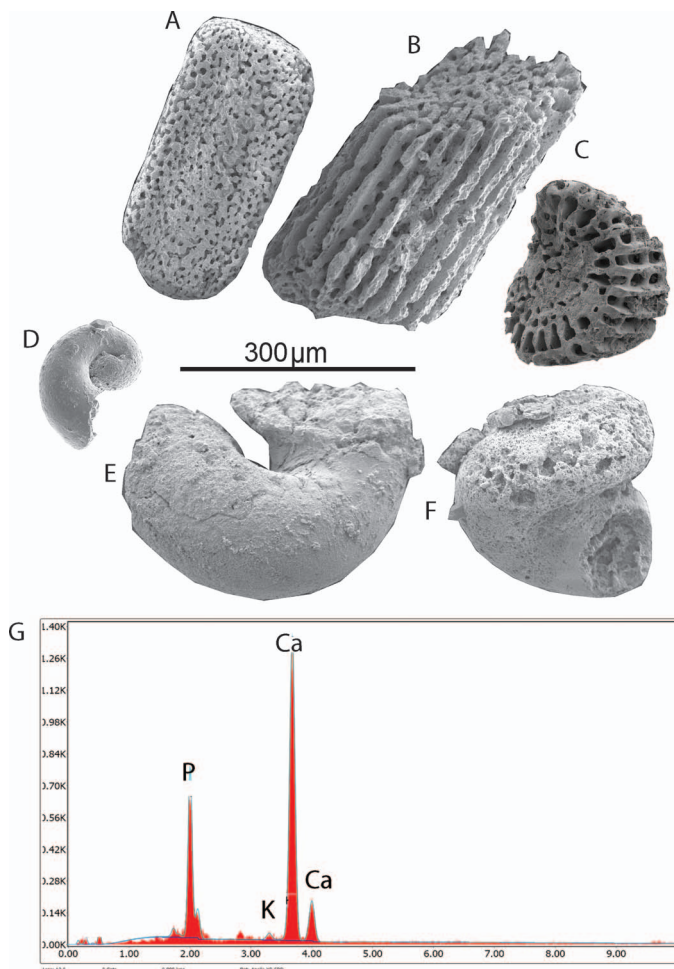Muddy Mountains Overton

Muddy Mountains Ute

FIG. 2.—Scanning electron microscope (SEM) images of stereomic molds of echinoderm fragments (A–C) and steinkerns of gastropods (D–F) from the Virgin Limestone Formation preserved by apatite. Representative EDS spectra of apatite shown in G (from gastropod in D), with gold and palladium peaks removed.

and the California Ridge near Ute in southern Nevada (Fig. 1; Shorb 1983; Pruss et al. 2005). It is constrained to latest Early Triassic (Spathian Stage) in age based on ammonoid biostratigraphy (Poborski 1954).

The Virgin Limestone Member has been well studied for its fossil community composition in the aftermath of mass extinction (Schubert and Bottjer 1995; Fraiser and Bottjer 2007), the abundance of microbialites (e.g., Schubert and Bottjer 1992; Pruss and Bottjer 2004; Mata and Bottjer 2011), and its silicified faunas (Moffat and Bottjer 1999). In the more proximal sections of the Virgin Limestone Member in the Muddy Mountains, silicified fossils occur in the upper half of these sections (Pruss et al. 2015). In six of these beds, fossils exhibiting small shelly style preservation are preserved.

METHODS

A set of 23 samples of fossil packstone and grainstone with silicified fossils were dissolved in 200–400 mL 10% glacial acetic acid solution

buffered with ammonium acetate. In six samples, insoluble residues of small size (250 μm to 420 μm; 177 μm to 250 μm) produced replaced skeletons and stereomic molds of echinoderms and internal molds of gastropods. Insoluble residues were examined under a Nikon SMZ645 stereoscopic microscope, and fossils with well-preserved morphology and exhibiting different mineralogical compositions were selected for further analysis. Each fossil was placed on a peg, coated with gold and palladium by a Hummer V Sputter Coater, and imaged with the FEI Quanta 450 Scanning Electron Microscope at Smith College. We also used EDS (Energy Dispersive Spectroscopy) Team software in conjunction with the 15 kV and 20 kV acceleration voltage to analyze the elemental composition of fossils by point analysis; several points were analyzed for each fossil to confirm consistency of composition, but only representative spectra are shown here.

We used powder X-ray diffraction (XRD) to determine the mineralogical composition of the residues that hosted the fossils. Because bulk powders were not analyzed by XRD reported mineralogical analyses refer to absolute amounts of the diagenetic minerals in our samples, rather than mineral abundances of the bulk rock. These analyses were performed at the University of Oxford on the insoluble residues of all sieved samples that preserved replaced small shelly style fossils. Powder X-ray diffraction was performed on these samples by grinding by hand in an agate mortar and pestle. Samples were mounted as a slurry mixed with anhydrous ethanol on a low background scattering silicon crystal substrate and analyzed using a Panalytical Empyrean Series 2 diffractometer operating at 40 kV and 40 mA with a Co Kα source. Samples were analyzed while continuously rotated and data were acquired from 5–85 degrees 2-theta using a step size of 0.026 degrees. Diffraction data were reduced using the HighScore Plus software suite and mineral identifications were based on correspondence to the ICDD Powder Diffraction File 4+ database. In addition, clay mineral speciation and polytype identification were performed by scanning from 69–75 degrees 2-theta using a step size of 0.026 degrees and count rates of 200 seconds per step. In this way, mineral-specific 060 reflections were quantified and clay mineral abundances expressed as a relative fraction of the total clay content, because the area of these reflections has been shown to correspond in a linear fashion to clay mineral abundance (Środoń et al. 2001).

RESULTS

Silicified fossils were found in 11 of the residues, but glauconitized and phosphatized fossils were only present in six of the dissolved samples. These fossils are preserved in the small size fractions of the insoluble residues (250 μm to 420 μm; 177 μm to 250 μm), and are rare or absent in any size fractions > 420 μm. Although glauconite and apatite are visibly present in many of the small sized residues, they occur as grains and do not always produce molds of fossils. Other grains that are glauconitized and phosphatized include ooids and grapestones, but these were not considered in this analysis. Silicified fossils also rarely occur in the small size fractions and are not as abundant as they were in the larger fractions.

The dominant fossils consist of echinoid spines with stereomic molds of apatite or glauconite and internal molds of gastropods (Figs. 2, 3). Forams, crinoid ossicles, and ophiuroid fragments are rare. The abundance of gastropod steinkerns is a common feature of small shelly style deposits from other intervals of time (e.g., Dzik 1994; Dattilo et al. 2016). Other fossils that were more commonly silicified, such as bivalves (Pruss et al. 2015), are not preserved by glauconite or apatite in these residues or were

---

←

FIG. 1.—Locality map and stratigraphic columns. **A**) Map showing location of the outcrops of the Virgin Limestone Member (36°36′01N, 114°32′57W, Muddy Mountains (MM) Overton locality; 36°32′51N, 114°36′50W, Muddy Mountains Ute locality). **B**) Stratigraphic columns showing all dissolved samples with location of small-shelly fossil samples in bold.
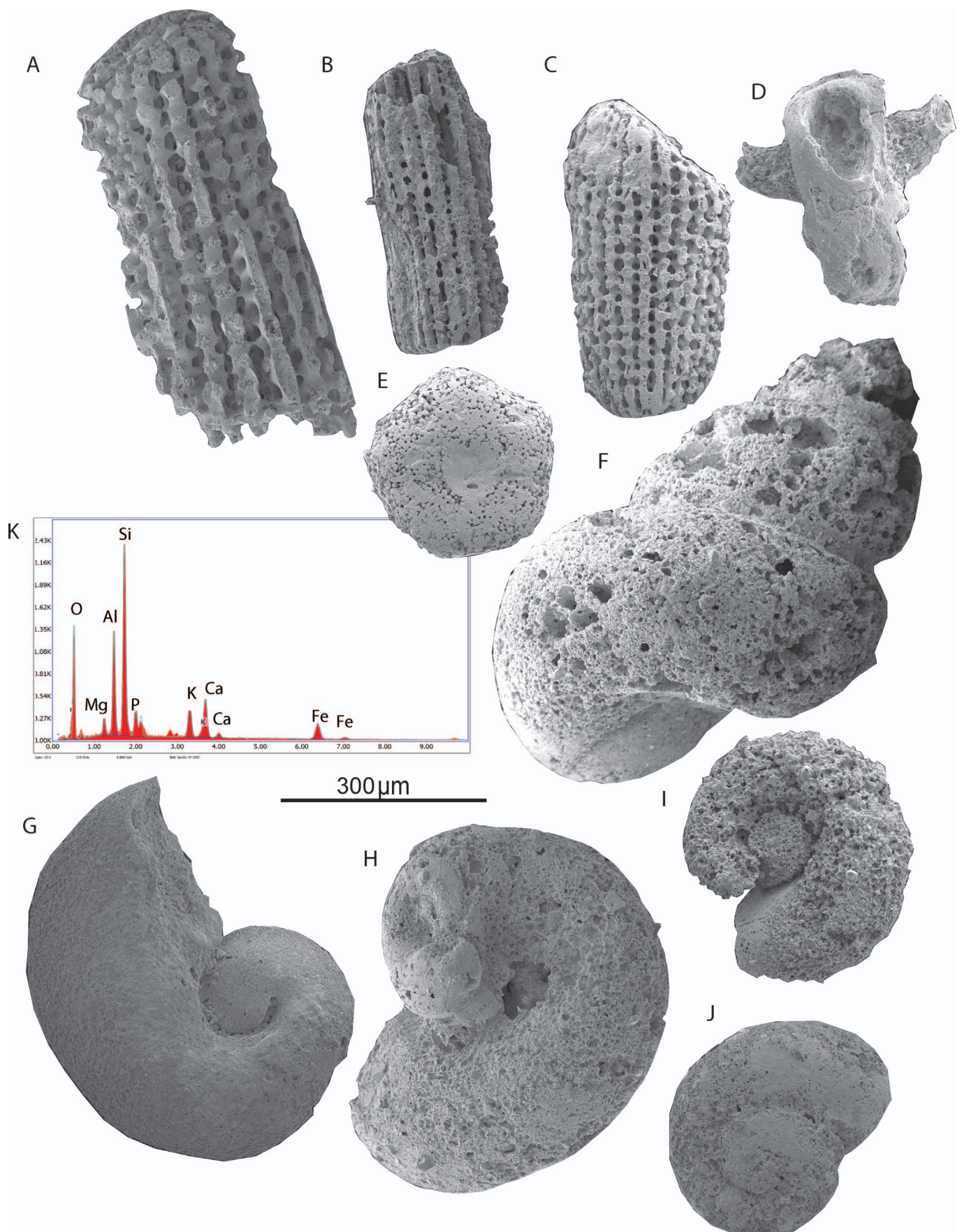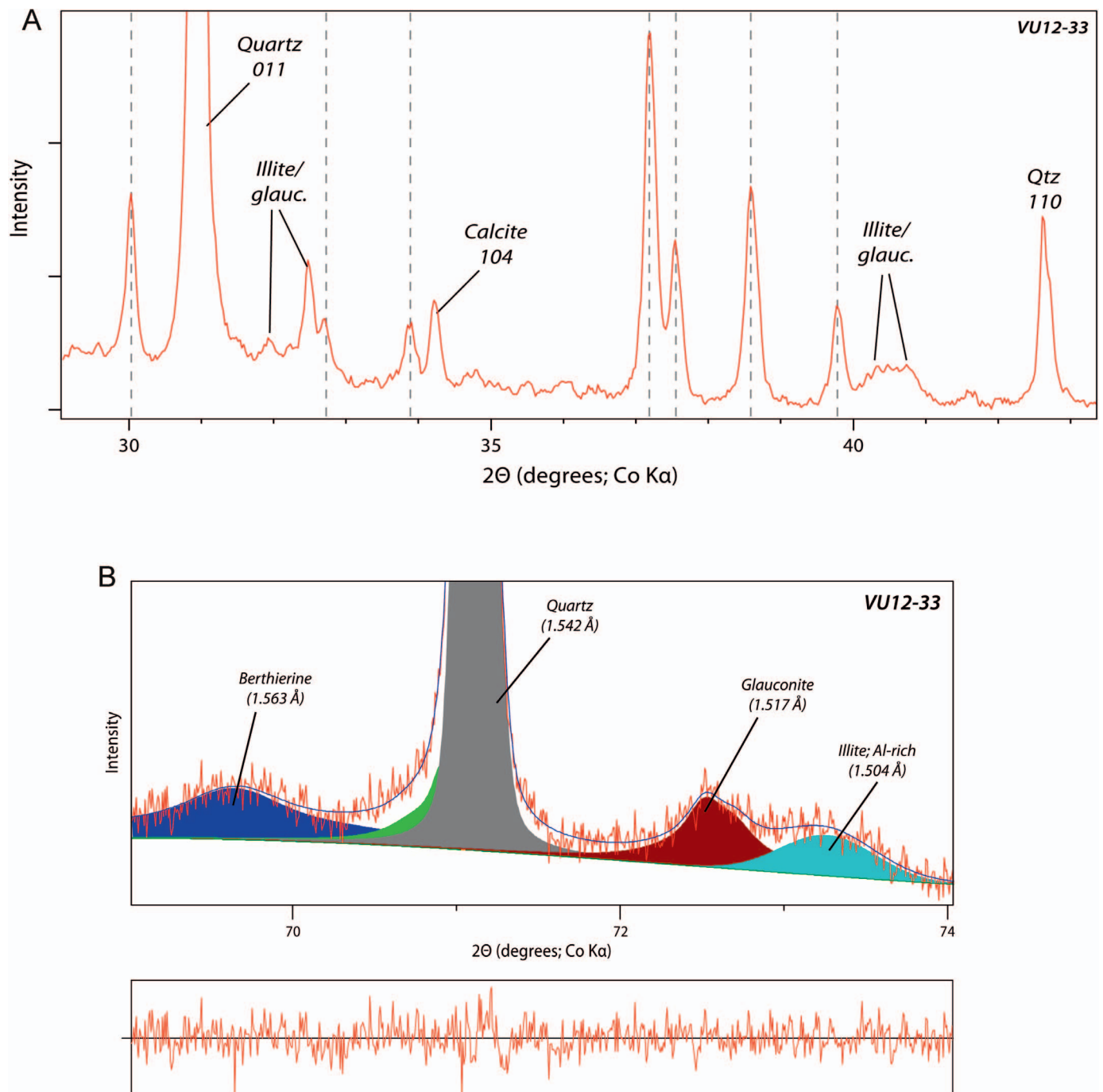
FIG. 4.—Identification of minerals in Virgin Limestone residues by X-ray diffraction (XRD). **A**) XRD profile from sample VU12-33 showing high abundances of glauconite (indicated) and apatite (dashed lines). Quartz and calcite peaks are also indicated. **B**) Zoomed in XRD profile from sample VU12-33 showing how glauconite, illite, and berthierine are identified. Quartz peak is also indicated.

too fragmented to identify. Most echinoderm material consists of broken skeletal plates and spines likely from crinoids and echinoids. Both planispiral and high-spired gastropods are present, but the granular preservation makes identification beyond class level difficult.

Both EDS (energy-dispersive spectra) of individual fossils and XRD of the residues confirm the mineralogic assignments (Figs. 2, 3). Pink or brown fossils, like an analyzed gastropod and echinoderm spine, typically had large peaks at Ca and P (Fig. 2), suggesting a composition of

---

←

FIG. 3.—Scanning electron microscope images of echinoderm spines (A–C), an ophiuroid fragment (D), a crinoid columnal (E), internal molds of gastropods (F–I), and a foraminiferan (J) from the Virgin Limestone Formation preserved, at least in part, by glauconite. Representative EDS spectra of glauconite is shown in K (from foraminiferan in J), with gold and palladium peaks removed. Small peaks of Ca and P show presence of apatite as well.

TABLE 1.—*X-ray diffraction (XRD) data for the six residues that produced abundant phosphatized and glauconitized fossils. Apatite and/or glauconite are present in all residues.*

Sample	Quar	Calc	Dolo	Apat	Illite	Glauc	Kaol	Goet	Pyr	Plag	Berth
VU12-33	37	2		16	7	10	Tr			22	6
VMM12-38	83	1	5	4	5	1					
VMM12-42	90	1	1	4	Tr	1		3			
VMM16-46A	55	1			21	23		1			Tr
VMM12-46B	25		64	4	3	2			Tr		2
VMM16-48A	69	21		8	Tr	Tr	Tr	3			

dominantly apatite. Green fossils generally had peaks in EDS spectra corresponding to Si, O, Al, Mg, K, and Fe with some Ca and P (Fig. 3). The presence of all of these elements is consistent with glauconite; the calcium and phosphorous peaks suggest apatite is also present. X-ray diffraction analysis of the residues that hosted the fossils reveal the presence of glauconite and apatite, and that they are each absent in only one residue (VMM12-42 and VMM16-46A, respectively; Fig. 4, Table 1); however, these minerals are never a major component of the insoluble residues (making up at most 23% of the fossiliferous residue). Other minerals of varying abundance include quartz and plagioclase with trace amounts of goethite, pyrite, and kaolinite (Table 1).

DISCUSSION

Echinoderm fragments and gastropods are the most common small shelly fossils of the Virgin Limestone Member, and these occur in the 250 μm to 420 μm and 177 μm to 250 μm size fractions. Generally, most fossils fall in the size range of 80 μm to ∼ 700 μm at their longest dimension; the smallest dimension of most small shelly style fossils is typically ∼ 100 μm. Interestingly, and unlike the Cambrian small shellies, small shelly style fossils in Lower Triassic rocks are remnants of taxa that are also preserved as large fossils. This indicates that this taphonomic window does not necessarily capture an unknown diversity as it does in the Cambrian but rather simply reflects the reemergence of a style of preservation that has rarely been reported from rocks deposited after the Paleozoic (Dzik 2004). The fragments preserved by glauconite and apatite are members of the same groups (crinoids, echinoids, ophiuroids, and gastropods) that are described from Early Triassic ecosystems globally, and it seems likely that this style of preservation can occur at any time that environmental conditions are conducive to it (Creveling et al. 2014b).

The Role of Redox Oscillations in Fossil Preservation

Small shelly style preservation has been extensively documented from rocks of the Cambrian (Brasier 1990; Dzik 1994; Porter 2004), and to a lesser degree in Ordovician deposits (Dattilo et al. 2016) and the remainder of the Paleozoic (Dzik 1994). In particular, globally widespread phosphatic deposits characterize the Ediacaran and Cambrian periods, including the Doushanto Formation; some of these exceptionally preserve fossils (e.g., Zhang et al. 1998). Small shelly fossils are essentially unknown from the post-Paleozoic fossil record, and previous authors have attributed this pattern to the closing of a taphonomic window that allowed for the preservation of fossils in this way (Porter 2004). In the Lower Triassic Virgin Limestone Member, the abundance of phosphatized and glauconitized fossils suggest a local return to Cambrian style preservation in these units. But what factors might have contributed to the re-opening of this taphonomic window in the Lower Triassic?

The presence of small shelly style fossils in Lower Triassic carbonates suggests an intermittent return to Cambrian-style diagenesis (e.g., Pruss et al. 2004, 2005). Recent work on the taphonomy of Cambrian small shelly fossils from Australia showed that steinkerns commonly form through phosphatization (Creveling et al. 2014b) by remobilization of phosphorous under locally anoxic conditions (Creveling et al. 2014a). In addition to the phosphatic fossils found in the Virgin Limestone, there is also an abundance of glauconitized fossils. The occurrence of both glauconite and apatite provides important constraints on the nature of pore water geochemistry, mineralization, and SSF preservation in the Virgin Limestone.

The abundant occurrence of glauconite, a redox-sensitive Fe-rich authigenic clay mineral, reflects the initial precipitation of Fe-rich smectite from pore water, and redox conditions that oscillated between oxic and anoxic. These prerequisites for glauconite formation arise because as Fe in authigenic Fe(II)-smectite is oxidized and then re-reduced in response to redox fluctuations, irreversible structural alterations act to increase K content, and increase Fe(II) content, which together act to decrease interlayer expandability (Khaled and Stucki 1991; Shen and Stucki 1994; Gorski et al. 2013; Neumann et al. 2011). Thus, with each oscillation in pore water redox, authigenic Fe-smectite precursors become progressively converted to glauconite (Khaled and Stucki 1991; Shen and Stucki 1994), the rate of which is a direct function of the rate of redox oscillation. From this perspective, it is easier to understand why, as discussed above, fluctuations in redox state of the interiors of organic-rich particles of a given size range are more likely to produce glauconite, at least in the presence of sufficient Fe, Mg and $SiO_2(aq)$ to promote the initial precipitation of Fe-smectite precursors. Indeed, glauconite is well known as an abundant and ubiquitous component of fecal pellets and irregular organic-rich grains and aggregates, highlighting a well-known mineralogical expression of the dynamic redox evolution of a wide variety of organic-rich microsystems (Boyer et al. 1977; Odin and Matter 1981).

The abundance of glauconite in particle interiors in turn provides crucial insight into the cycling of phosphate in Virgin Formation sediments, and therefore the precipitation of apatite. The phosphate localized in apatite was likely provided by P liberated from organic matter and/or from the shuttling of Fe, whereby adsorbed P on Fe-oxide particles is released and locally concentrated where redox cycling occurs (Berner 1973; Krom and Berner 1981; Slomp et al. 1996). Indeed, a sedimentary Fe source and oscillating redox reflected by glauconite would have amplified the efficiency of PO_4^{3-} delivery and concentration in small shelly microenvironments through redox cycling. In addition to Fe-associated PO_4^{3-}, previous work has shown that oscillating redox tends to promote P storage in organic matter, relative to fully anoxic sediments (Aller 1994). Together, redox oscillations would have promoted increased PO_4^{3-} concentrations in particle interiors from both Fe-associated and organic-associated sources.

Although redox oscillations were clearly important in concentrating PO_4^{3-} at the local scale in Virgin Limestone SSFs, the precipitation of carbonate-fluoro-apatite (CFA) requires the availability of CO_3^{2-}, which is closely coupled to pH. On the basis of this requirement, Creveling et al. (2014b) suggested that, in the presence of sufficient sedimentary PO_4^{3-} sources, relatively low SO_4^{2-} concentrations would have helped promote

CFA nucleation because greater proportions of reducible Fe relative to SO_4^{2-} would promote enhanced Fe reduction, in turn increasing pore water pH, making CO_3^{2-} more available, and increasing CFA supersaturation. The abundance of glauconite perhaps reflects a greater role for Fe reduction in buffering pore water pH relative to SO_4^{2-} reduction, in particular if marine SO_4^{2-} concentrations were lower in the Triassic than modern seawater (Song et al. 2014). Although modern diagenetic studies indicate that redox oscillations may have promoted complex dynamic changes in the availability of oxidants and in pore water pH (Zhu et al. 2006), low pore-water SO_4^{2-} may have been a key prerequisite that helped promote the formation of apatite in addition to glauconite in Virgin Limestone SSFs.

In summary, glauconite and apatite associated with SSFs indicate that redox oscillations within shell interiors played a key role in generating both minerals. Redox fluctuations drove glauconitization of precursor Fe-smectite, which itself reflects an important source of Fe to Virgin Limestone sediments. These fluctuations enhanced PO_4^{3-} accumulation in shell interiors through redox cycling of particulate Fe minerals and/or the preferential accumulation, and eventual release, of P associated with organic matter.

Size Selection of Early Triassic Small Shelly Style Fossils

The echinoderms have stereom filled in by apatite and glauconite, often in the same samples where the larger fractions hosted silicified examples (Pruss et al. 2015). It is possible that the abundance of organic matter in the stereom, which has been known to play a role in silicification of fossils, fostered glauconitization and phosphatization of echinoderms in these assemblages, (e.g., Butts 2014; Butts and Briggs 2010; Pruss et al. 2015). However, there must be other factors at play because glauconitized and phosphatized fossils are nearly absent from the larger size fractions ($>$ 420 µm). The gastropods follow a similar pattern of preservation to early Paleozoic small shelly assemblages with an abundance of steinkerns in these Triassic residues (Creveling et al. 2014b; Dattilo et al. 2016). The steinkerns are thought to reflect external sources of phosphate (Wilby and Briggs 1997), with some nucleation on existing organic material (Creveling et al. 2014a, 2014b). The preservation of these fossils in the smallest size fractions suggests that selectivity relating to size is operating (Creveling et al. 2014b) even relative to silicified fossils in the same assemblages (silicified fossils are typically 1 mm or larger).

One way to understand why SSF preservation in the Virgin Limestone is associated with a size selection is to consider the controls on the redox state of the interior of the shells or fossils themselves. Following Jorgensen (1977), Jahnke (1985) constructed a simple model to interpret pore-water profiles of oxygen and nitrogen species in deep-sea sediments by treating particles containing organic matter as simple spheres. In this model, the redox state of the interior (or, more precisely, the conditions for anoxia to develop at the center of the particle) is a function of the effective radius of the particle (R), the diffusion coefficient within the particle (D, or the value incorporating chemical diffusivity across organic membranes, etc.), the $O_2(aq)$ content of the surrounding pore water (C), and the rate of $O_2(aq)$ consumption within the particle (J), which is determined by the net rate of $O_2(aq)$-consuming metabolic reactions for a given microbial ecology. Anoxia will develop in the center of the particle following the equation:

$$R = (6DC/J)^{1/2}$$

Figure 5 plots this relationship at two different pore water $O_2(aq)$ concentrations. It is clear from this relationship that, for any given rate of $O_2(aq)$ consumption and $O_2(aq)$ content of the surrounding pore water, there will be a size limit above which the interior of the particle will be continuously anoxic. Similarly, particles that are below a given $O_2(aq)$ consumption rate, or below the resolution of our analytical techniques, will be continuously oxic or be characterized by a redox state identical to

that of the surrounding pore water. This is simply because particles below a given size limit do not contain enough organic matter to overcome the diffusion of $O_2(aq)$ from surrounding pore water to the particle center. However, particles within these two end member sizes will be characterized by redox conditions that are poised close to the anoxic/oxic boundary. It follows that oscillations in the redox state of the interiors of particles within this size range will be likely to occur in response to small variations in any combination of local $O_2(aq)$ content, metabolic $O_2(aq)$ consumption rate, or changes in the diffusivity of the interior. Importantly, Figure 5 also shows that as the $O_2(aq)$ concentration of the pore water decreases, so too does the particle size window at which redox oscillations are likely to occur. Thus, lower pore water $O_2(aq)$ selects for smaller particle sizes (like those that fall in the size ranges of the SSF's reported here) that are more likely to experience redox oscillations during deposition and early diagenesis. In this scenario, if a fossil fragment is not spherical, maximum O_2 consumption rates will occur along the smallest dimension of a fossil fragment, not the largest; this is simply because the diffusive length scale is shortest along the shortest fossil axis. Therefore, compared to well-oxygenated pore waters, low ambient pore water oxygen will subject smaller particles to more frequent redox oscillations. Figure 5 illustrates this relationship in the case where low pore-water O_2 imposes redox oscillations on particles with their smallest dimension within the size range of $\sim$ 80 µm to $\sim$ 350 µm (capturing the majority of our fossil occurrences).

These simple calculations examining the development of particle anoxia indicate that low $O_2(aq)$ in sediment pore water exerted a size selection on particles likely to experience redox oscillations at a given metabolic ($O_2(aq)$ consumption) rate. In addition, low marine, and therefore, low pore-water SO_4^{2-} concentrations, combined with sufficient reducible sedimentary Fe, allowed pH to increase upon microbial mineralization of organic matter. This, in turn, allowed CO_3^{2-} concentrations to rise, driving increased supersaturation of CFA in the particles themselves. Together, these conclusions imply that SSF preservation during Virgin Limestone sedimentation and diagenesis was, above all else, a strong function of low pore-water $O_2(aq)$ and low SO_4^{2-}.

It is possible, in light of the fossils preserved here, that there are other intervals of the Phanerozoic that might contain fossils preserved in a similar way. For example, in addition to the abundance of glauconitic and phosphatic deposits of the Cambrian, the Cretaceous contains abundant glauconite worldwide (Peters and Gaines 2012). Local examples show widespread glauconite associated with phosphorites during warm, low oxygen conditions (Glenn and Arthur 1988). Since warm epicontinental seas were occasionally present throughout the Cretaceous, this may be yet another interval that contains small shelly style preservation of fossils, given that conditions were right for glauconitic and phosphatic deposits.

Environmental Conditions of the Early Triassic

The end-Permian mass extinction triggered a delayed recovery for five million years following the event (e.g., Erwin 2001), and this interval of time is characterized by long-term environmental stress. For example, the Early Triassic experienced large-scale oscillations in the carbon isotope record potentially linked to periodic volcanism (Payne and Kump 2007), lethally hot ocean temperatures (Sun et al. 2012), and evidence for sustained anoxia (e.g., Isozaki 1997; Grice et al. 2005; Grasby et al. 2013). Lower Triassic glauconitic and phosphatic deposits are known from high-latitude successions, like the Vardebukta (Wignall et al. 1998) and Vikinghøgda formations (Mørk et al. 1999) of Svalbard, and lesser amounts in low latitude outer shelf settings, like Aggtelek Karst, Hungary (Hips 1999), but they are quantitatively rare when normalized to rock volume and compared to other time intervals (Peters and Gaines 2012). Nonetheless, their presence in Lower Triassic successions points to
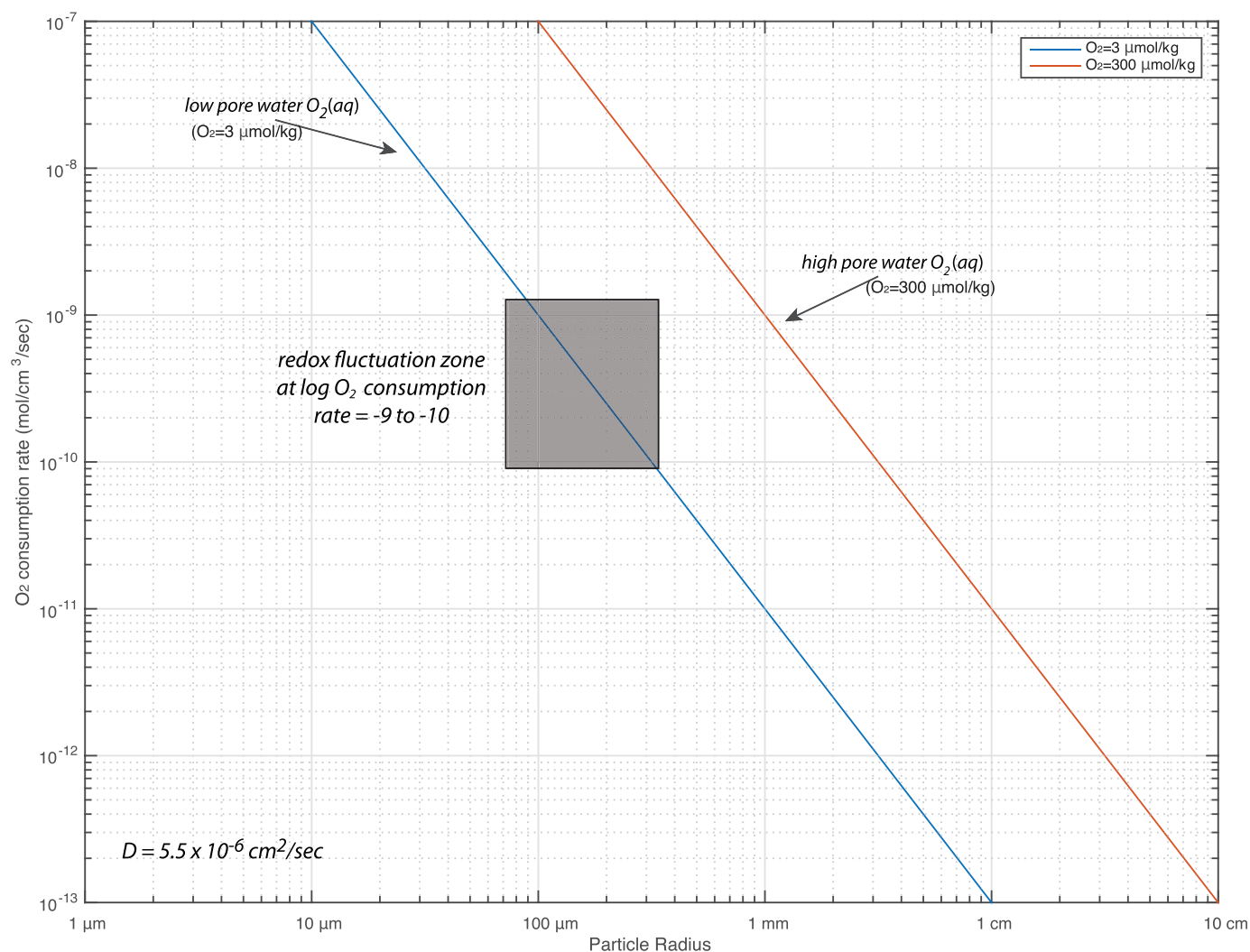
FIG. 5.—Diagram showing particle radius versus oxygen consumption rate using the model of Jahnke (1985), following Jorgensen (1977). Note that the size of small shelly style fossils in the Virgin Limestone assemblage fall along the region of redox fluctuations in an ambient low oxygen pore water environment.

conditions, at least in some areas, which were conducive to the formation of glauconitic and phosphatic deposits.

It is generally accepted that offshore environments of the Early Triassic experienced low oxygen conditions, perhaps for millions of years (e.g., Isozaki 1997; Grice et al. 2005; Grasby et al. 2013; Song et al. 2014). What has been less well-known is the degree to which low-oxygen waters affected shelf environments, and reports have put forth equivocal views (e.g., Twitchett et al. 2004; Lau et al. 2016). Here, the presence of glauconitized and phosphatized fossils in these facies suggests that the sediments of the Lower Triassic Virgin Limestone experienced oscillating redox during early diagenesis after burial, which, in turn, fostered small shelly style preservation. In addition to oscillating background oxygen levels, Lower Triassic sediments have been widely viewed as poorly ventilated because of conspicuously low levels of bioturbation (Buatois and Mángano 2011), related to small trace fossils coupled with low ichnofabric indices (Pruss and Bottjer 2004). Other indicators of suppressed animal activity include the preservation of wrinkle structures and other microbialites worldwide (Pruss et al. 2004). We prefer the notion that poorly ventilated sediments allowed for redox oscillations rather than local organic loading, since shallow water sections of the Lower Triassic,

including the units examined here, are notoriously lean with respect to organic carbon (Krull et al. 2004; Marenco et al. 2012). Small shelly style fossilization in these Triassic sediments indicates that environmental conditions that also brought about a long-term delayed recovery from the end-Permian mass extinction promoted diagenetic reactions that controlled the styles of fossilization.

CONCLUSIONS

Small shelly fossils of the Lower Triassic Virgin Limestone offer valuable insight into the specific diagenetic conditions that controlled the spatial and temporal distribution of this taphonomic mode. The mineralogical composition of these fossils unambiguously reflects periodically low oxygen content of sediment pore waters. Because these conditions persisted for five million years beyond the end-Permian mass extinction, Lower Triassic carbonates offer a new opportunity to examine the diagenetic consequences of Earth's largest mass extinction and its delayed recovery. Finally, the resurgence of small shelly style fossils in the Lower Triassic helps explain the closing of this taphonomic window in the Cambrian. Global geochemical datasets reflect a shift to oxygenated conditions well into the later Paleozoic (Sperling et al. 2015), so as

seafloors became progressively ventilated, redox oscillation became less common and so too did the early diagenetic precipitation of glauconite and/or apatite—mineral substrates that each reflect a dynamic sedimentary redox landscape.

REFERENCES

ALLER, R.C., 1994, Bioturbation and remineralization of sedimentary organic matter: effects of redox oscillation: Chemical Geology, v. 114, p. 331–345

ALLISON, P.A. AND BRIGGS, D.E.G., 1993, Exceptional fossil record: distribution of soft-tissue preservation through the Phanerozoic: Geology, v. 21, p. 527–530.

BERNER, R.A., 1973, Phosphate removal from sea water by adsorption on volcanogenic ferric oxides: Earth and Planetary Science Letters, v. 18, p. 77–86.

BOYER, P.S., GUINNESS, E.A., LYNCH-BLOSSE, M.A., AND STOLZMAN, R.A., 1977, Greensand fecal pellets from New Jersey: Journal of Sedimentary Research, v. 47, p. 267–280.

BRASIER, M. L., 1990, Phosphogenic events and skeletal preservation across the Precambrian–Cambrian boundary interval: Geological Society of London, Special Publications, v. 52, p. 289–303.

BUATOIS, L. A. AND MÁNGANO, M. G., 2011, The déjà vu effect: Recurrent patterns in exploitation of ecospace, establishment of the mixed layer, and distribution of matgrounds: Geology, v. 39, p. 1163–1166.

BUTTS, S.H., 2014, Silicification, in M. LaFlamme, J.D. Schiffbauer, and S.A.F. Darroch (eds.), Reading and Writing of the Fossil Record: Preservational Pathways to Exceptional Fossilization: Paleontological Society Short Course, v. 20, p. 15–33.

BUTTS, S.H. AND BRIGGS, D.E., 2010, Silicification through time, in P. Allison and D.J. Bottjer (eds.), Taphonomy: Process and Bias Through Time: Springer, Berlin, p. 411–434.

CREVELING, J.C., JOHNSTON, D.T., POULTON, S.W, KOTRC, B., MARZ, C., SCHRAG, D.P., AND KNOLL, A.H., 2014a, Phosphorus sources for phosphatic Cambrian carbonates: Geological Society of America Bulletin, v. 126, p. 145–163.

CREVELING, J.C., KNOLL, A. H., AND JOHNSTON, D. J., 2014b, Taphonomy of Cambrian small shelly fossils: PALAIOS, v. 29, p. 295–308.

DATTILO, B., FREEMAN, R.L., PETERS, W.S., HEIMBROCK, W.P., DELINE, B., MARTIN, A.J., KALLMEYER, J.W., REEDER, J., AND ARGAST, A., 2016, Giants among micromorphs: were Cincinnatian (Ordovician, Katian) small shelly phosphatic faunas dwarfed?: PALAIOS, v. 31, p. 55–70.

DZIK, J., 1994, Evolution of 'small shelly assemblages' of the early Paleozoic: Acta Palaeontologica Polonica, v. 39, p. 247–313.

ERWIN, D.H., 2001, Lessons from the past: biotic recoveries from mass extinctions: Proceedings of the National Academy of Sciences, v. 98, p. 5399–5403.

FRAISER, M.L. AND BOTTJER, D. J., 2007, When bivalves took over the world: Paleobiology, v. 33, p. 397–413.

GLENN, C.R. AND ARTHUR, M.A., 1988, Petrology and major element geochemistry of Peru margin phosphorites and associated diagenetic minerals: authigenesis in modern organic-rich sediments: Marine Geology, v. 80, p. 231–67.

GORSKI, C.A., KLÜPFEL, L.E., VOEGELIN, A., SANDER, M., AND HOFSTETTER, T.B., 2013, Redox properties of structural Fe in clay minerals, 3, relationships between smectite redox and structural properties: Environmental Science and Technology, v. 47, p. 13477–13485.

GRASBY, S.E., BEAUCHAMP, B., EMBRY, A., AND SANEI, H., 2013, Recurrent Early Triassic anoxia: Geology, v. 41, p. 175–178.

GRICE, K., CAO, C., LOVE, G.D., BÖTTCHER, M.E., TWITCHETT, R.J., GROSJEAN, E., SUMMONS, R.E., TURGEON, S.C., DUNNING, W., AND JIN, Y., 2005, Photic zone euxinia during the Permian–Triassic superanoxic event: Science, v. 307, p. 706–709.

HIPS, K., 1999, Lower Triassic storm-dominated ramp sequence in northern Hungary: an example of evolution from homoclinal through distally steepened ramp to Middle Triassic flat-topped platform: Geological Society of London Special Publications, v. 159, p. 315–338.

ISOZAKI, Y., 1997, Permo–Triassic boundary superanoxia and stratified superocean; records from lost deep sea: Science, v. 276, p. 235–238.

JAHNKE, R., 1985, A model of microenvironments in deep-sea sediments: formation and effects on porewater profiles: Limnology and Oceanography, v. 30, p. 956–965.

JØRGENSEN, B. B., 1977, Bacterial sulfate reduction within reduced microniches of oxidized marine sediments: Marine Biology, v. 41, p. 7–17.

KHALED, E.M. AND STUCKI, W., 1991, Iron oxidation state effects on cation fixation in smectites: Soil Scientific Society of America Journal, v. 55, p. 550–554.

KROM, M.D. AND BERNER, R.A., 1981, The diagenesis of phosphorus in a nearshore marine sediment, Geochimica et Cosmochimica Acta, v. 45, p. 207–216.

KRULL, E.S., LEHRMANN, D.J., DRUKE, D., KESSEL, B., YU, Y., AND LI, R., 2004, Stable carbon isotope stratigraphy across the Permian–Triassic boundary in shallow-marine carbonate platforms, Nanpanjiang Basin, south China: Palaeogeography, Palaeoclimatology, Palaeoecology, v. 204, p. 297–315.

LAU, K.V., MAHER, K., ALTINER, D., KELLEY, B.M., KUMP, L.R., LEHRMANN, D.J., SILVA-TAMAYO, J.C., WEAVER, K.L., YU, M., AND PAYNE, J.L., 2016, Marine anoxia and delayed Earth system recovery after the end-Permian extinction: Proceedings of the National Academy of Sciences, v. 113, p. 2360–2365.

MARENCO, P.J., GRIFFIN, J.M., FRAISER, M.L., AND CLAPHAM, M.E., 2012, Paleoecology and geochemistry of Early Triassic (Spathian) microbial mounds and implications for anoxia following the end-Permian mass extinction: Geology, v. 40, p. 715–718.

MATA, S.A. AND BOTTJER, D.J., 2011, Origin of Lower Triassic microbialites in mixed carbonate-siliciclastic successions: Ichnology, applied stratigraphy, and the end-Permian mass extinction: Palaeogeography, Palaeoclimatology, Palaeoecology, v. 300, p. 158–178.

MØRK, A., ELVEBAKK, G., FORSBERG, A.W., HOUNSLOW, M.W., NAKREM, H.A., VIGRAN, J.O., AND WEITSCHAT, W., 1999, The type section of the Vikinghøgda Formation: a new Lower Triassic unit in central and eastern Spitsbergen: Polar Research, v. 18, p. 51–82.

MOFFAT, H. A. AND BOTTJER, D. J., 1999, Echinoid concentration beds: two examples from the stratigraphic spectrum: Palaeogeography, Palaeoclimatology, Palaeoecology, v. 149, p. 329–348.

NEUMANN, A., SANDER, M., AND HOFSTETTER, T.B., 2011, Redox properties of structural Fe in smectite clay minerals: Aquatic Redox Chemistry: ACS Symposium Series, American Chemical Society, Washington, DC, p. 361–379.

ODIN, G.S. AND MATTER, A., 1981, De glauconiarum origine: Sedimentology, v. 28, p. 611–641.

PAYNE, J.L. AND KUMP, L.R., 2007, Evidence for recurrent Early Triassic massive volcanism from quantitative interpretation of carbon isotope fluctuations: Earth and Planetary Science Letters, v. 256, p. 264–277.

PETERS, S. E. AND GAINES, R. 2012, Formation of the 'great unconformity' as a trigger for the Cambrian explosion: Nature, v. 484, p. 363–366, doi:10.1038/nature10969.

POBORSKI, S.J., 1954, Virgin Formation (Triassic) of the St. George, Utah, area: Geological Society of America Bulletin, v. 65, p. 971–1006.

PORTER, S.M., 2004, Closing the phosphatization window: testing for the influence of taphonomic megabias on the pattern of small shelly fossil decline: PALAIOS, v. 19, p. 178–183.

PRUSS, S.B. AND BOTTJER, D.J., 2004, Early Triassic trace fossils of the western United States and their implications for prolonged environmental stress from the end-Permian mass extinction: PALAIOS, v. 19, p. 559–571.

PRUSS, S.B., CORSETTI, F.A., AND BOTTJER, D.J., 2005, The unusual sedimentary rock record of the Early Triassic: a case study from the southwestern United States: Palaeogeography, Palaeoclimatology, Palaeoecology, v. 222, p. 33–52.

PRUSS, S.B., FRAISER, M.L., AND BOTTJER, D.J., 2004, Proliferation of Early Triassic wrinkle structures: implications for environmental stress following the end-Permian mass extinction: Geology. v. 35, p. 461–465.

PRUSS, S.B., PAYNE, J.L., AND WESTACOTT, S., 2015, Taphonomic bias of selective silicification revealed by paired petrographic and insoluble residue analysis: PALAIOS, v. 30, p. 620–626.

SCHUBERT, J.K. AND BOTTJER, D.J., 1992, Early Triassic stromatolites as post-mass extinction disaster forms: Geology, v. 20, p. 883–886.

SCHUBERT, J.K. AND BOTTJER, D.J., 1995, Aftermath of the Permian–Triassic mass extinction event: paleoecology of Lower Triassic carbonates in the Western USA: Palaeogeography, Palaeoclimatology, Palaeoecology, v. 116, p. 1–39.

SHEN, S. AND STUCKI, J., 1994, Effects of iron oxidation state on the fate and behavior of potassium in soils: Soil Testing: Prospects for Improving Nutrient Recommendations: Soil Science Society of America, SSA Special Publication 40, p. 173–85

SHORB, W.M., 1983, Stratigraphy, facies analysis and depositional environments of the Moenkopi Formation (Lower Triassic), Washington County, Utah, and Clark and Lincoln counties, Nevada: Unpublished MS thesis, Duke University, Durham, North Carolina, 205 p.

SLOMP, C.P., VAN DER GAAST, S.J., AND VAN RAAPHORST, W., 1996, Phosphorus binding by poorly crystalline iron oxides in North Sea sediments: Marine Chemistry, v. 52, p. 55–73.

SONG, H., TONG, J., ALGEO, T.J., SONG, H., QIU, H., ZHU, Y., TIAN, L., BATES, S., LYONS, T.W., LUO, G., AND JKUMP, L.R., 2014, Early Triassic seawater sulfate drawdown: Geochimica et Cosmochimica Acta, v. 128, p. 95–113.

SPERLING, E.A., WOLOCK, C.J., MORGAN, A.S., GILL, B.C., KUNZMANN, M., HALVERSON, G.P., MACDONALD, F.A., KNOLL, A.H., AND JOHNSTON, D.T., 2015, Statistical analysis of iron geochemical data suggests limited late Proterozoic oxygenation: Nature, v. 523, p. 451–454.

ŚRODOŃ J., DRITS V.A., MCCARTY D.K., HSIEH J.C., AND EBERL, D.D., 2001, Quantitative x-ray diffraction analysis of clay-bearing rocks from random preparations: Clays and Clay Minerals, v. 49, p. 514–528.

SUN, Y., JOACHIMSKI, M.M., WIGNALL, P.B., YAN, H., CHEN, Y., JIANG, H., XANG, L., AND LAI, X., 2012, Lethally hot temperatures during the Early Triassic: Science, v. 338, p. 366–370.

TWITCHETT, R.J., KRYSTYN, L., BAUD, A., WHEELEY, J.R., AND RICHOZ, S., 2004, Rapid marine recovery after the end-Permian mass-extinction event in the absence of marine anoxia: Geology, v. 32, p. 805–808.

WIGNALL, P.B., MORANTE, R., AND NEWTON, R., 1998, The Permo–Triassic transition in Spitsbergen: $\delta^{13}C_{org}$ chemostratigraphy, Fe and S geochemistry, facies, fauna and trace fossils: Geological Magazine, v. 133, p. 47–62.

WILBY, P.R. AND BRIGGS, D.E.G., 1997, Taxonomic trends in the resolution of detail preserved in fossil phosphatized soft tissues: Geobios, v. 30, p. 493–502.

ZHANG, Y., LEIMING Y., XIAO, S., AND KNOLL, A.H., 1998, Permineralized fossils from the terminal Proterozoic Doushantuo Formation, South China: Journal of Paleontology, v. 72, p. 1–52.

ZHU, Q., ALLER, R.C., AND FAN, Y., 2006, Two-dimensional pH distributions and dynamics in bioturbated marine sediments: Geochimica et Cosmochimica Acta, v. 70, p. 4933–4949.